Complexin-1 Regulated Assembly of Single Neuronal SNARE Complex Revealed by Dual-Trap Optical Tweezers

Tongrui Hao (haotongrui2018@sibcb.ac.cn)
Center for Excellence in Molecular Cell Science https://orcid.org/0000-0002-4237-5666
Nan Feng
Fan Gong
Yang Yu
Jiaquan Liu
Yu-Xuan Ren

Article

Keywords:

Posted Date: March 8th, 2022

DOI: https://doi.org/10.21203/rs.3.rs-1400492/v1

Running title: Single molecule study of SNARE with Optical tweezers

Complexin-1 regulated assembly of single neuronal SNARE complex revealed by dual-trap optical tweezers

Tongrui Hao[1,2,*], Nan Feng[1,2], Fan Gong[3], Yang Yu[3], Jiaquan Liu[1,*], Yu-Xuan Ren[4,*]

[1]*State Key Laboratory of Molecular Biology, Shanghai Institute of Biochemistry and Cell Biology, Center for Excellence in Molecular Cell Science, Chinese Academy of Science, Shanghai 200031, China;*

[2]*University of Chinese Academy of Sciences, Beijing, 200049, China;*

[3]*National Facility for Protein Science in Shanghai, Zhangjiang Lab, Shanghai Advanced Research Institute, Chinese Academy of Sciences, Shanghai 201210, China;*

[4]*Institute for Translational Brain Research, Shanghai Medical College, Fudan University, Shanghai 200032, China;*

Correspondence to TH (haotongrui2018@sibcb.ac.cn), JL (liujiaquan@sibcb.ac.cn), or YR (yxren@fudan.edu.cn)

Abstract

The dynamic assembly of the Synaptic-soluble N-ethylmaleimide-sensitive factor Attachment REceptor (SNARE) complex is crucial to the membrane fusion. Traditional ensemble studies lack the information of dynamic assembly of the protein complex. Here, we apply minute force on a tethered protein complex through dual-trap optical tweezers and study the folding dynamics of SNARE complex under mechanical force regulated by complexin-1 (CpxI). We reconstructed the clamp and facilitate functions of CpxI in vitro. Specially, the 1-83 amino acids (aa) of CpxI mainly implement the facilitate function, while the N-terminal domain (NTD) plays a dominant role. CTD is mainly related to Clamping, and separate 1-83aa and C-terminal domain (CTD) of CpxI can efficiently

reconstitute the inhibitory signal identical to that the full-length CpxI functions. Our observation identifies the important chaperone role of the CpxI molecule in the dynamic assembly of SNARE complex under mechanical tension, and elucidates the specific function of each fragment of CpxI molecules in the chaperone process. Additionally, the developed technique may also be applied to study the mechanobiology and folding dynamics of single molecular protein complex.

Introduction

The neurotransmitter release and intercellular communication requires the membrane fusion, which takes place within a millisecond[1]. The membrane fusion is driven by crucial fusion proteins, such as the molecular machine Synaptic-soluble N-ethylmaleimide-sensitive factor Attachment REceptor (SNARE) proteins. Meanwhile, many regulatory proteins, such as N-ethylmaleimide sensitive factor (NSF), soluble NSF adaptor proteins (SNAPs), Complexin (Cpx) and synaptotagmin-1, are involved in the regulation of SNARE zippering and are crucial for the membrane fusion to efficiently occur at the precise time in vivo [2,3]. However, the functions of many important regulators have not been well understood in single-molecule level. Traditional ensemble-based approaches are not able to dissect the dynamic assembly of SNARE, and are insufficient to record the less populated misassembled states[4,5]. In addition, functional SNARE assembly occurs in the presence of the opposing force imposed by membranes, which has a great impact on the kinetics and regulation of SNARE assembly [6,7].

Although SNARE assembly has been studied using the soluble SNAREs isolated from membranes, the lack of an essential force may complicate data interpretation regarding functional SNARE assembly. Single molecule optical tweezers can apply mechanical force with high precision and low photodamage on biological molecules, and can measure force and distance in real time. Although the single neuronal SNARE complex zipper in three distinct stages [6], it is still unclear on how the dynamic SNARE assembly is regulated by many proteins, e.g., complexin. As a small cytosolic α-helical protein [8], Cpx can bind on the SNARE complex, and executes unique functions [9]. Cpx

either acts as a clamp to inhibit the release to maintain a proper primed vesicle pool [9], or facilitates Ca^{2+}-triggered synchronous neurotransmitter release. We use single-molecule optical tweezers to study the Cpx regulated SNARE assembly, and dissect the dynamic conformational change and force-dependent intermediate states under mechanical force. In this condition, the SNARE complex maintained a four-state transition and the CpxI binding site can be identified from single molecule experiment. We further identified the function of CpxI in the whole zippering process. The interplay of the CpxI with individual functional SNARE complex during dynamic transition under mechanical tension would be identified through dual-trap optical tweezers to record the dynamic assembly of the SNARE complex [10,11]. The indirect capture of a single protein molecule/complex allows the study of the dynamics under mechanical tension. Such single molecule technique is not only a tool complementary to the ensemble methods, but also can detect many important and less populated intermediates involved in the protein function.

Results

Dual-trap optical tweezers with sophisticated control

The optical tweezers were invented by A. Ashkin in 1986, who won the Nobel Prize in Physics in 2018 because of the invention of optical tweezers and the application in biology. The application of optical tweezers spans from colloidal physics, cell biology, to single molecule biophysics. Specifically, for single molecule biophysics, we built the dual-trap optical tweezers to exert minute force on a tethered protein complex (Figure

1a). The dual-trap optical tweezers, built on a concrete background, adopt differential detection to minimize the systematic noise coupled from the environment [11-13]. The laser source is a continuous wave laser with center wavelength at 1064 nm (J20I-BL-206C, customized with 10m fiber bundle, Spectra-Physics). The laser was isolated from the back reflection with an electro-optic isolator (IO-3-1064-VHP, Thorlabs) to prevent damage and destabilization to the laser cavity. A half-wave plate (HW1) in combination with a polarizing beam splitter (PBS1) controls the total power delivered to the dual-trap optical tweezers. A second half-wave plate (HW2) adjusts the power ratio between two laser traps. The first telescope expands the beam into ~ 4 mm in diameter. The expanded beam was then split and combined by a pair of polarization beam splitters (PBS2 and PBS3). One beam will be kept fixed, while the other beam is steered using a movable mirror driven by a piezostage (Nano-MTA2X, MadCity Labs Inc). A second telescope T2 expands the beam diameter by twice and relayed the piezomirror to the back focal plane (BFP) of the trapping objective (OB1, NA=1.2, UPLSAPO60XWIR-2, Olympus). Here, in order to maximize the detection efficiency, we adopted two identical objectives (OBJ1 and OBJ2) for trapping and detection. Both objectives are optimized for high transmission (>80%) at the trapping wavelength (1064 nm).

The position detection was performed through two position sensitive detectors (PSDs, DL100-7 PCBA3, Pacific silica) conjugated at the BFP of the detection objective (OB2). To assist for the experiment, a bright-field microscope was co-aligned with the dual-trap optical tweezers. The bright field illumination was provided by a laser emitting diode (LED), and monitored in real time through a charge coupled device camera (CCD)

(scA640-74fc, Basler). The two laser traps were created by focusing two orthogonally polarized 1064 nm laser beams (Fig. 1a) with a high transmission water-immersion objective. Two microspheres in the trap act as force and displacement sensors. The position traces were detected through two PSDs conjugated to the BFP of the detection objective with back focal plane interferometry[14]. The dual-trap optical tweezers were installed inside an isolated room from environmental noise with well temperature control and air conditioning, specifically, the temperature fluctuation is below 1 ℃, while the air flow speed is smaller than 0.1 m/s at the outlet of the air conditioning system. To minimize the noise from human operation and noisy instrument, the laser controller with fan was moved outside of the room with a multimode fiber bundle to deliver pump light into the laser cavity, and the instrument is operated, e.g., addition of sample, tether formation, calibration, and measurement, outside the room through Labview interface. The instrument operated in high resolution passive mode, with the location of two traps kept stationary during the recording. Once an increase of the applied force was required, the movable trap separates more from the stationary one through the piezomirror.

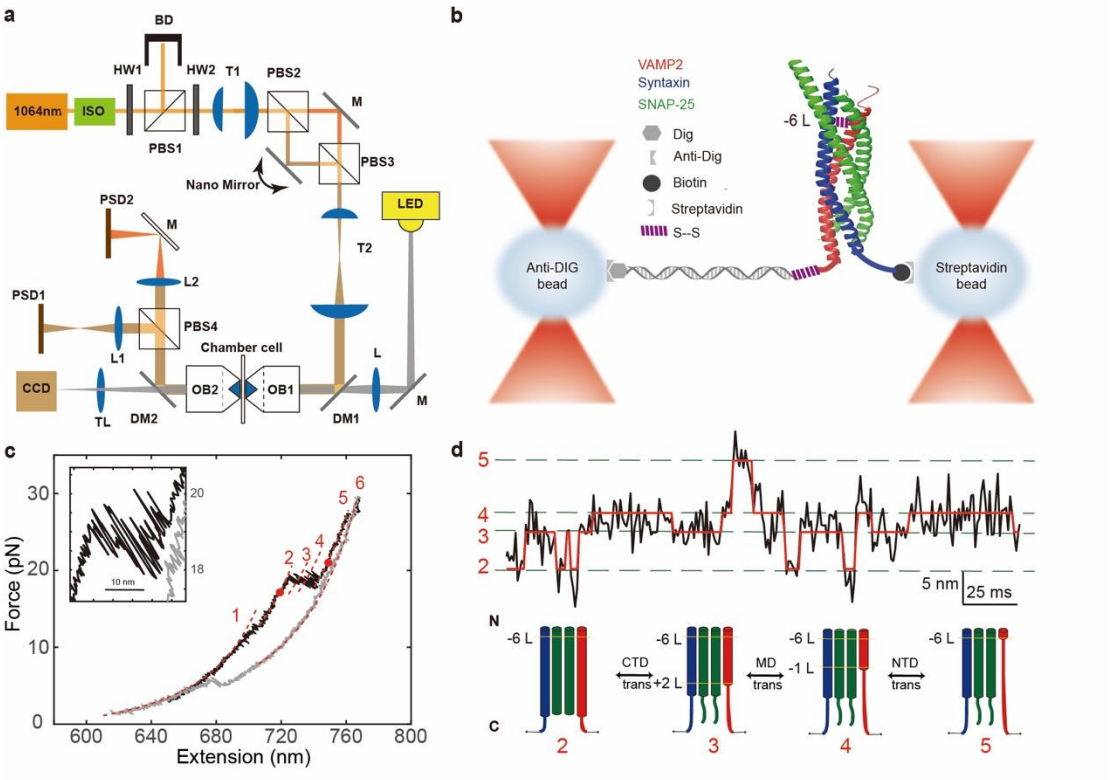

Figure 1. Schematics of single molecule study with dual-trap optical tweezers. a Layout of dual-trap optical tweezers. The trapping beam comes from a solid-state laser with central wavelength of 1064 nm. ISO, isolator; HW, half-wave plate; BD, Beam Dump; T, telescope; PBS, polarizing beam splitter; OBJ, water immersion objective; L, lenses; TL, tube lens; PSD, position sensitive detector; LED, laser emitting diode; DM, dichroic mirror. b Schematics of the single molecule essay. The preassembled SNARE complex was crosslinked to a 2,260-bp DNA handle through disulfide bond and further attached with two microspheres through either digoxigenin/anti-digoxigenin or biotin/streptavidin. c Force-extension curves (FECs) of a single SNARE complex during pulling (black) and relaxing (gray). The continuous regions of the FECs corresponding to different assembly states (marked by red numbers) were fitted using the worm-like chain model (red lines). The inset shows a close-up view of the region

marked by two red dots. d Extension-time trajectories of single SNARE complexes under constant trap separation. The ideal state transitions derived from hidden-Markov model (HMM) are expressed in red lines. The positions of different states are marked by green dashed lines and labeled with the state numbers. Data were filtered using a time window of 0.2 ms. SNARE configurations correspond to the states in extension-time trajectories, black numbers and L (-6 L, +2 L) indicate different layers (-6 layer, +2 layer).

To observe reversible and regulatory SNARE assembly, we designed SNARE complexes containing the full cytoplasmic domain and a crosslinking site between syntaxin and VAMP2 (synaptobrevin-2) near the -6 hydrophobic layer (Fig. S3). The SNARE proteins were purified independently, then assembled into SNARE complexes in vitro (Fig. S1). We identified that CpxI does not bind to any SNARE monomers, but do bind to the SNARE complex (Fig. S2). A 2,260-bp DNA handle containing an activated thiol group at its 5'end was added to the solution of SNARE complex with a molar ratio of 1:20. Intramolecular and intermolecular crosslinking occurred in open air between the cysteine residues on syntaxin and VAMP2 and between VAMP2 and the DNA handle. The DNA handle contains two digoxigenin moieties at the 3' end. Both the thiol group and digoxigenin moieties on the handle were introduced in the PCR through primers. During the single molecule experiment, the SNARE complex was tethered through DNA handle between anti-dig and streptavidin beads through the

dual-dig and biotin tag (Fig. 1b).

We use dual-trap optical tweezers to capture two microspheres. One microsphere coated with the protein-DNA complex is kept stationary, while the other with streptavidin coating is movable to approach the stationary microsphere to form a tether. Once the tether is detected, the movable trap separates from the stationary trap to a certain distance to apply force on the tether of the DNA handle connected with the protein. To manipulate a single SNARE complex, we either pulled or relaxed the complex by moving one optical trap relative to the other at a constant speed (typically of 20 nm/s) or held the complex under constant trap separation. Both force and extension of the protein-DNA complex were recorded at 10 kHz. When the force rises to 7~13 pN, we observe a ~3 nm slow hopping (between states 1 and 2 in Fig. 1c) corresponding to the opening of the liner domain of the SNARE complex [6,10]. The SNARE transits from fully zippered/folded state 1 to linker-open state 2 when the linker domain is dissembled. However, when the force increases to 17~19 pN [6], the SNARE complex hops among four states with maximum extension difference of ~20 nm (Fig.1c) [6,10,15] because the SNARE complex is cross-linked to -6 layer. Thus, the complete dissociation of the SNARE complex at the N-terminal (state 3-5) does not occur immediately after the assembly of the SNARE complex at the C-terminal (state 2-3). In this case, the slow dissociation of SNARE complex's four helix bundle is represented by the continuous hopping signal (between state 2 to 5 in fig. 1c). And there is a dissociation of the Middle domain (MD) of the SNARE complex (states 3-4) near the central ion layer (0 layer). When the force continues increasing, a rip signal of ~5 nm appeared (between state 5

to 6 in fig. 1c), indicating the irreversible dissociation of SNAP25, the last monomer without disulfide bond. When the force gradually decreases below 5 pN, the SNARE complex could not return to full assembly in the absence of SNAP25 in the solution (Fig.1c, gray curve). The time-dependent extension and force were mean-filtered using a time window of 7 ms. The Force-extension curve of the handle DNA would be fitted using Worm-like chain model [16] (dashed curve in Fig. 1c).

CpxI clamp partially folded SNARE complex

To characterize CpxI-dependent SNARE assembly/disassembly, we measured the extension-time trajectories at a certain average force where SNARE transits among 4 states (Fig. 2a). Firstly, we captured SNARE complex and stretched it for a cycle to check correct assembly of the SNARE complex molecule and to determine the equilibrium force of intermediate state. The equilibrium force is generally between 18 and 20 pN. The overall distribution of different SNARE molecules' equilibrium force approximates a normal distribution, which has been corroborated for all the measured SNARE complex. We fixed the optical trap separation to apply a constant trap separation at the equilibrium, the SNARE complex would transit among 4 states (2-5, Fig. 1d).

Cpx consists of four domains, N-terminal domain (NTD), accessory helix (AH), center helix (CH) and C-terminal domain (CTD) (inset in Fig. 2a). The crystal structure of Cpx/SNARE complex and mutagenesis experiments have revealed that the CH is

directly associated with SNAREs, which is essential for Cpx to execute function [17,18]. We held individual SNARE complex by dual-trap optical tweezers with a fixed trap separation, and supplied 8 μM CpxI in a separate channel ('protein channel') to directly inject the CpxI to the region where the SNARE folding/unfolding took place. In the presence of 8 μM full-length CpxI, 37 SNARE complex changed their state after the addition of CpxI. For 33% of them (12 molecules), the distribution of SNARE complexes changed from 2~5 states to 3~5 states (Fig. 2a-d), which implies that the reversible assembly and disassembly is limited to N-terminal. Moreover, we further stretched these molecules, and found that their FEC curves also changed significantly compared with those in the absence of CpxI (Fig. 2d). Most SNARE complex couldn't zip completely even the force dropped below 5 pN (Fig. 2d, C-terminal clamped state, cyan line), suggesting that CpxI might insert into the C-terminal of SNARE and inhibit the complete zippering of SNARE complex (Fig. 2a-d). HMM analysis of extension-time trajectories for single SNARE complexes also suggests that the SNARE complex was locked to the C-terminal blocked state in the presence of 8 μM full length CpxI (1-134 aa) (Fig. 2c). This signal corresponds to CpxI's clamp function in physiological state.

We also observed that SNARE complex could be clamped by CpxI into the exactly half-zippered state (6 molecules, 16% signal rate, Fig. 2a, 2b, 2d). Accordingly, the dynamic folding of SNARE complex is limited to 3~4 states. We continue to stretch this complex by ramping up the force, and find that it requires a higher force to break this half-zippered state. This corroborates that CpxI can inhibited the C-terminal assembly of

SNARE complexes, and simultaneously stabilize the N-terminal. This also corresponds to CpxI's clamp function in physiological state.

Additionally, The SNARE complex can also maintain in linker-open state after the addition of CpxI (19 molecules, 51% signal rate, Fig. 2a, 2b, 2d). Accordingly, SNARE complexes have changed from hopping among 2-5 states to being maintained only in the second state with the addition of CpxI. Further stretching of the molecules requires a high force to break this linker-open state, indicating the ability of CpxI to stabilize the four-helix bundle of SNARE complexes. This is necessary for CpxI to assist in the zippering of SNARE complex when the Ca^{2+} arrived in a physiological state, which also represents the function of facilitate.

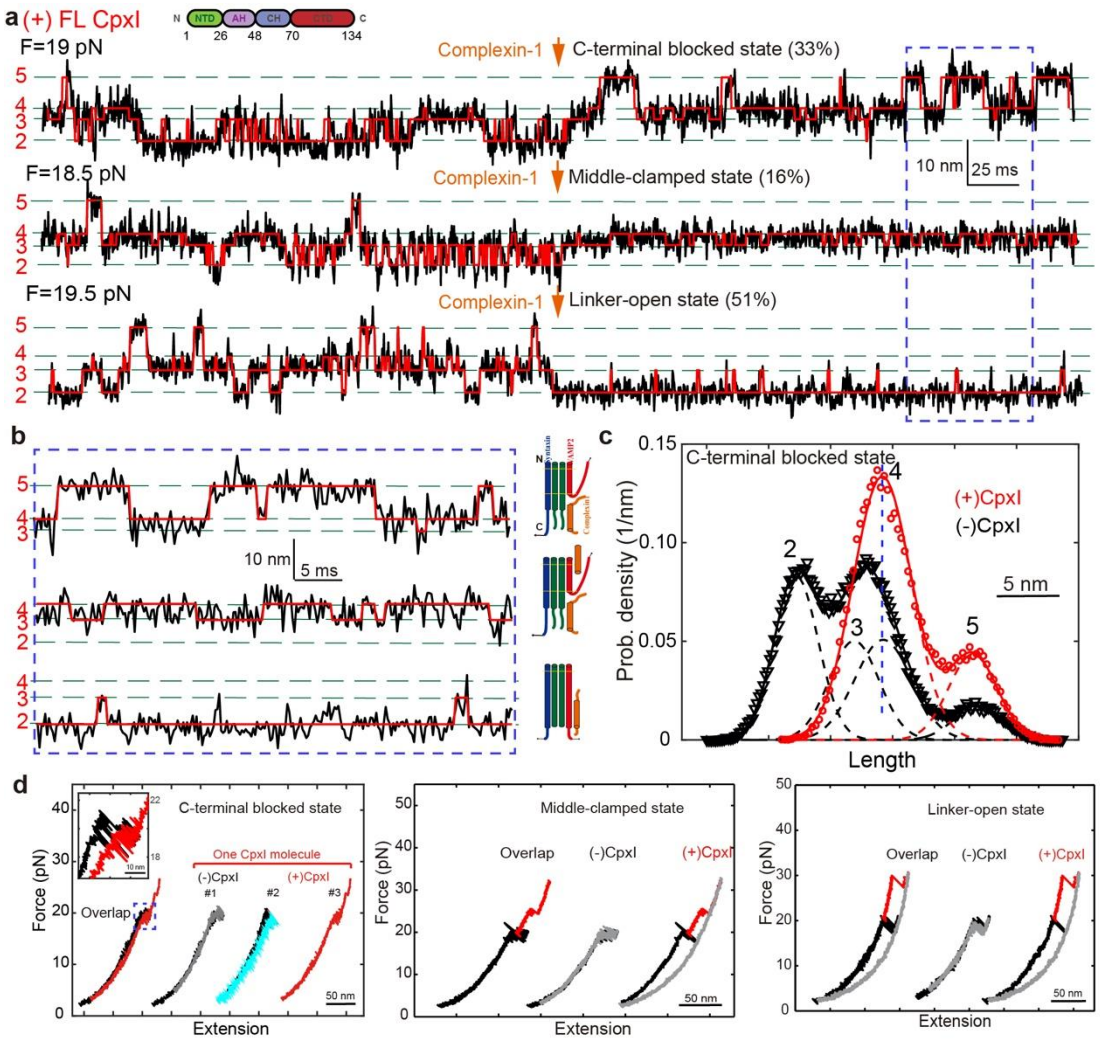

Figure 2. CpxI stabilizes partially folded SNARE complex. a Extension-time trajectories of single SNARE complexes under constant trap separation in the presence of CpxI. The arrow indicates the administration of 8 μM full-length CpxI molecules. The ideal state transitions derived from hidden-Markov model (HMM) are expressed in red lines. The positions of different states are marked by green dashed lines and labeled with the state numbers. Data were filtered using a time window of 0.2 ms. b Close-up views of the region marked by dashed blue rectangles. c SNARE configurations correspond to the states in b, black numbers and L (-6 L, +2 L) indicate

different layers (-6 layer, +2 layer). d Probability distributions of the extensions corresponding to the traces in a in the presence (red circle) and the absence (black triangle) of CpxI and their best fits by a sum of four Gaussian functions (red and black lines). e FECs of a single SNARE complex before (black) and after (red) the addition of 8 μM CpxI, and cyan line is the relaxing FEC after the addition. The FECs of the different cycles generally overlap but were shifted along x-axis for clarity. The inset shows a close-up view of the region in dashed blue rectangle.

Moreover, in the process of consecutive rounds when pulling and relaxing the same SNARE complex, the possibility of the same signal appearing in the subsequent cycle after a certain signal is higher than 80%, indicating that the same CpxI may be combined with the same SNARE in multiple cycles of pulling and relax (Fig. 2d).

CpxI 1-83aa stabilized the SNARE complex at linker-open state

To figure out the specific function of multiple domains in the CpxI-dependent SNARE transition dynamics, we introduced different truncations of CpxI to the single transitioned SNARE complex, including 1-83 aa, 26-83 aa, 48-73 aa, mixture of 1-83 aa and 83-134aa (Fig. 3a). Remarkably, we found that the signals of SNARE folding in presence of 1-83 aa (lack the NTD of CpxI compared to full-length CpxI) were the most consistent among all kinds of CpxI fragments. In the presence of 8 μM 1-83 aa of CpxI, 49 dynamic SNARE complex molecules changed their state after the addition of CpxI, when another 13 molecules showed no significant change after the addition. Interestingly, among these 49 SNARE complexes with significant configuration change,

94% (46 molecules) of their extension-time traces were stabilized at linker-open state, and higher force was required to further break the linker-open state (Fig. 3b). And other 3 SNARE complexes (6%) were limited into N-terminal transition. Obviously, the 1-83 aa domain of CpxI stabilizes the SNARE at linker-open state. In other words, 1-83 aa can only implement the facilitate function.

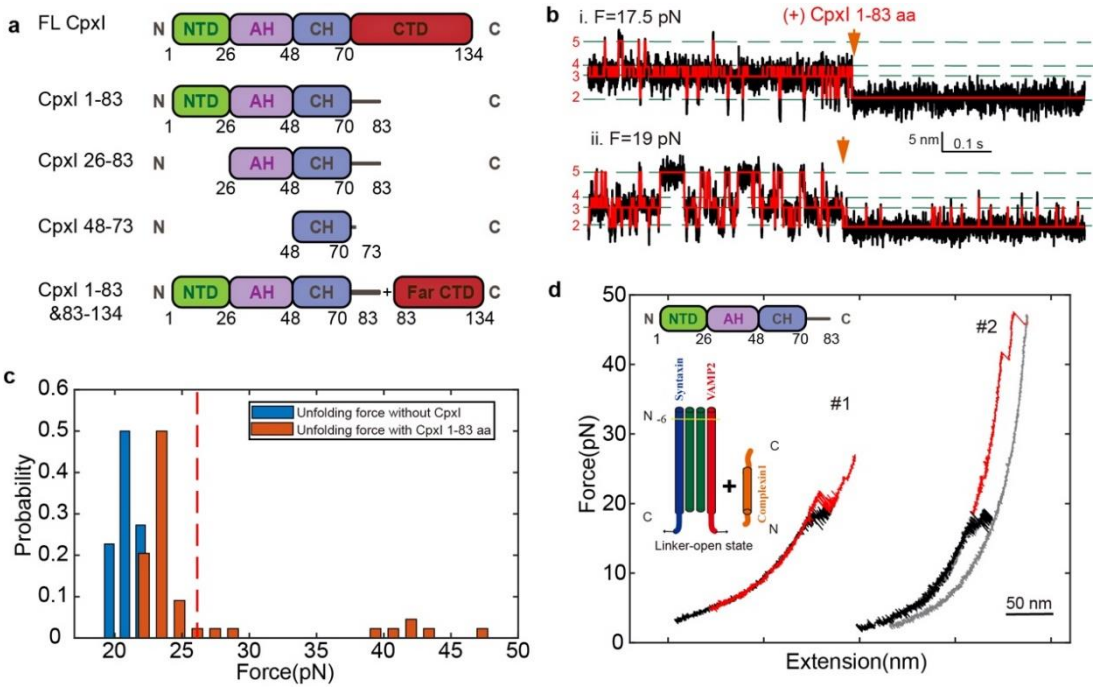

Figure 3. Fragment 1-83aa of CpxI stabilizes the SNARE complex at the linker-open state. a Schematics of the domain fragments in the CpxI used in the experiments. b Extension-time trajectories of single SNARE complexes under constant trap separation showing SNARE unfolding kinetics before and after the addition of 8 μM fragment 1-83aa of CpxI. c The distribution of the unfolding force of SNARE complexes with (orange) or without (blue) 1-83 aa fragments. d Force-extension curves (FECs) of a single SNARE complex before (black) and after (red) the addition of 8 μM 1-83aa. The

1-83 aa domain of CpxI stabilizes the SNARE assembly at the linker-open state, for which 59% of the FECs changed slightly with an increase of up to 5pN (#1) on the unzipped force of SNARE C-terminus, and 34% of the force-extension curve (FEC) changed dramatically with an increase of more than 5pN (#2) on the unzipped force of SNARE C-terminus.

The unfolding forces of the C-terminal in SNARE complexes are normally distributed around an average of ~ 21 pN (Fig. 3c). However, in the presence of CpxI, the unfolding forces of the C-terminal in SNARE complexes increased differently. In these liner-open state stabilized signals, the unzipping force of the C-terminal for 34% SNARE complexes under study increased by more than 5 pN (Fig. S5a), and the unzipping force for 59% of the C-terminal SNARE increased up to 5pN (Fig. 3c, d, Fig. S5b).

CpxI NTD stabilizes the four-helix bundle of SNARE complex

The NTD (1-26 aa) is an important domain of CpxI to stabilize the C-terminal of SNARE complex[19,20], specifically ability of CpxI to stabilize SNARE complex may mostly depend on its NTD. To pinpoint the possible role of the NTD in the CpxI - dependent SNARE disassembly, we removed the NTD in the CpxI construct. The NTD removal led to significant changes in disassembly of SNARE complex in the activation of Ca^{2+}-triggered neurotransmitter release. Interestingly, the NTD domain (1-26 aa) of CpxI may localize to the point where trans-SNARE complex insert into the fusing membranes [21], or lock the C-terminal of SNARE complex in the absence of Ca^{2+} [20,22].

These findings suggest that the in the presence of 8 μM CpxI 26-83 aa, 38 dynamic molecules changed their state after the addition of CpxI (Fig. 4a, 4b). Interestingly, the extension-time traces of 25 molecules (66%) were still stabilized at linker-open state (Fig. S6), while 12 SNARE complexes' C-terminal transition were blocked (31.5%, Fig. 4a, 4b). As for the latter signal, most SNARE complex also couldn't achieve complete zippering even the force dropped below 5 pN (Fig. 4c, cyan line). The rate of linker-open state decreased dramatically, showing that the removal of NTD caused significant changes in the CpxI-dependent SNARE disassembly (Fig. 4d), which indicates that the CpxI stabilizes the SNARE complex critically depending on its N-terminal domain (NTD, 1-26 aa). So NTD plays a leading role in the facilitate function.

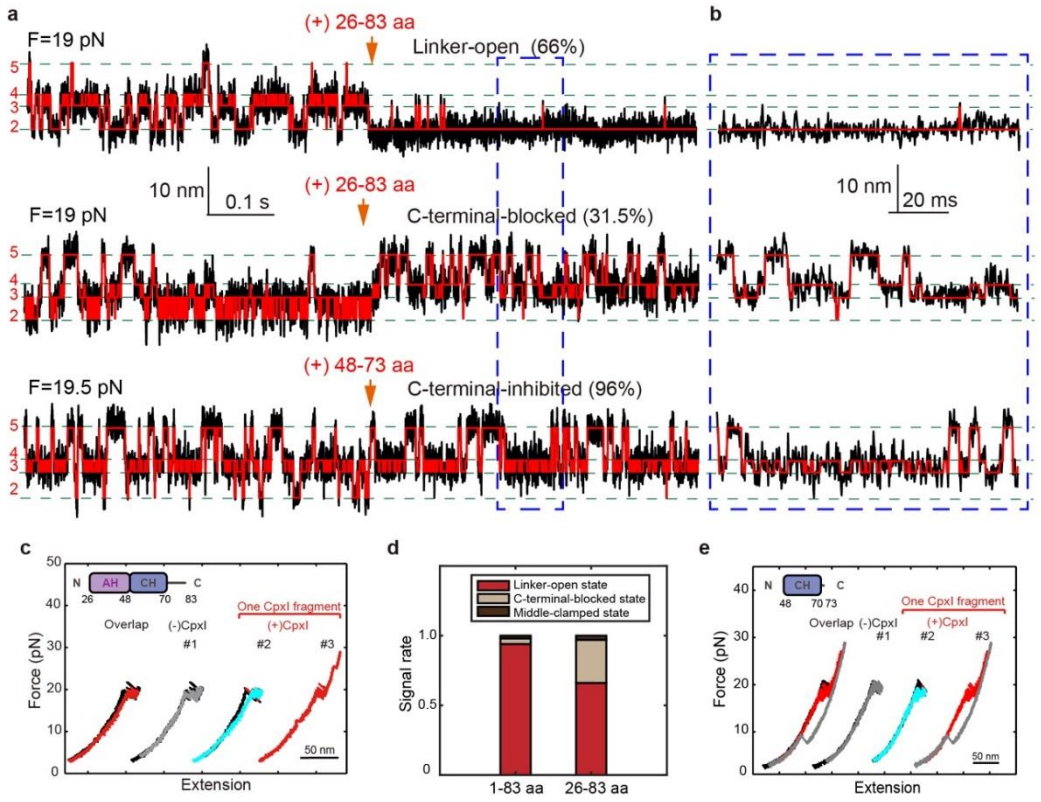

Figure 4. The stable function of CpxI NTD and Cpx CH domain can slightly inhibit the assembly of C-terminal of SNARE complex. In the presence of 8μM AH-CH domain (26-83 aa), 38 of 66 (57.5%) dynamic molecules changed their state after the addition of the CpxI fragment. a Extension-time trajectories and b zoom-in view of the traces in the dashed rectangle suggest that 66% of them was stabilized to linker-open state after the addition of 8 μM AH-CH domain (26-83aa) in real time, 31.5% of SNARE complex were locked at the C-terminal blocked state after (red) the addition of 8 μM AH-CH domain. For the addition of a shorter fragment of CH domain (8 μM 48-73aa), 26 of 32 (81%) dynamic molecules changed their state in the presence of CpxI fragment. c FEC curve, black: pulling before the addition of CpxI, gray: relaxing before the addition of Cpx, red: pulling after the addition of CpxI, cyan: relaxing after the addition of CpxI. d Summary of the distribution of the different kind of signals introduced by fragments of 1-83 aa or 26-83 aa. e FECs of single SNARE complexes in the presence of merely CH domain. 96% of the SNARE complex were locked to the C-terminal blocked state after (red) the addition of CpxI CH domain.

The CH domain (48-73 aa) of Cpx is believed to be the smallest fragment that directly binds with SNARE complex [21]. We supplied 8μM CH domain of CpxI to the single-molecule SNARE complex experiment, and found that the CpxI CH slightly inhibits the assembly of C-terminal of SNARE complex (Fig. 4a, 4b). Specifically, 26 molecules changed their state after the addition of CpxI, and 96% of their C-terminal transition were slightly blocked (25 molecules, Fig. 4e). However, these molecules showed full assembly as force decreases (the cyan line in Fig. 4e), quite different from

the effect of other longer CpxI fragments (the cyan line in Fig. 2f, 4c). A much shorter fragment of CpxI 48-73 aa is insufficient to clamp the SNARE complex into the linker-open state.

Structural studies can provide an insightful explanation. The crystal structures of Cpx: SNARE complex show different interaction surfaces when Cpx of different lengths is used. For Cpx 32-72 aa [23] or 24-73 aa [23]), the binding position of Cpx CH corresponds to the middle part of the SNARE complex (0 ~ +1 layer); for a shorter Cpx 49-76 aa (containing only CH) [18], the Cpx CH binds to the proximal C-terminal of the SNARE complex, When the Cpx peptide is too small, the binding position of CH moves towards the C-terminal of the SNARE complex. This suggests that if the Cpx fragment is too short (only CH), weak or even erroneous interactions are likely to occur, because the functional binding of Cpx requires the coordination of other Cpx domains. Our observation supports the hypothesis that CpxI AH-CH is the "minimum Clamp unit"[24].

CpxI CTD inhibits the C-terminal refolding and stabilizes the N-terminal folding of SNARE complex

Recent function analyses with C. elegans Cpx revealed that CpxI inhibitory effects is important but not sufficient for membrane binding [25,26], making it mysterious for the interactions of the Cpx C-terminus for arresting vesicle fusion. Hereby, we elucidate whether CTD is functional in the absence of phospholipid. CpxI CTD can't directly bind to SNARE in the absence of CH, and CTD fragment (83-134 aa) doesn't binding to 1-83 aa (Fig. S4). We introduce CTD fragment (83-134 aa) combined with 8 μM 1-

83 aa of CpxI to interact with the SNARE complex during dynamic assembly. This scheme is similar to the addition of full length CpxI, but each CpxI molecule is separated into two pieces. Unexpectedly, 18 SNARE complex molecules changed their states after the addition of 8μM 1-83 aa fragment and 8μM 83-134 aa (with molar ratio of 1:1); 21 SNARE complex molecules changed their state after the addition of 8 μM 1-83 aa and 16 μM 83-134 aa (molar ratio 1:2); 22 SNARE complex molecules changed their state after the addition of 8μM 1-83 aa and 24μM 83-134 aa (molar ratio 1:3) (Fig. 5a-c, Fig. S9). Different combinations of CpxI fragments lead to different types of signal distribution (Fig. 5c).

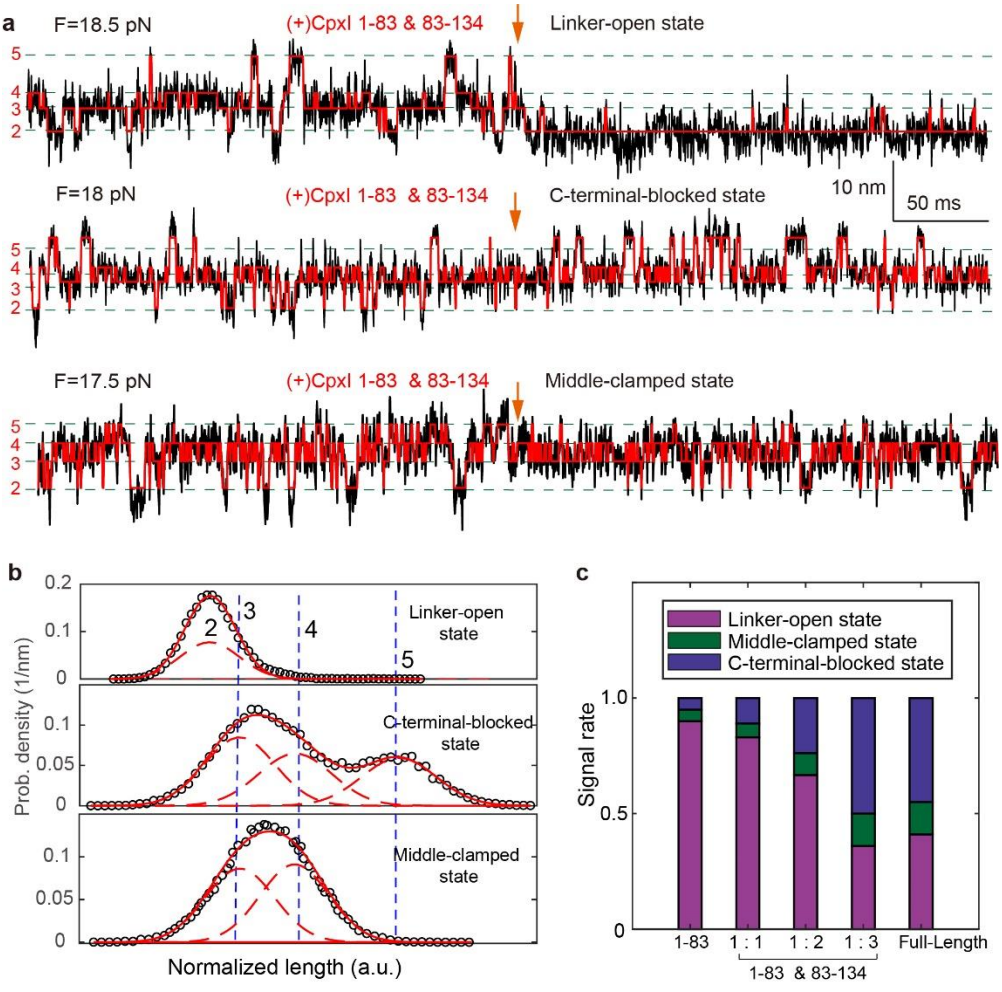

Figure 5. CpxI CTD can inhibit the assemble of C-terminal of SNARE complex and stabilize the N-terminal of SNARE complex. a Extension-time trajectories of single SNARE complexes show SNARE unfolding kinetics before (black) and after (red) the addition of 8 μM fragments of 1-83 aa and 8/16/24 μM fragments of 83-134 aa in real time. b Characteristic probability density distributions of the extensions corresponding to the traces in A and their best fits to a sum of four Gaussian functions (red lines). c The distribution of different kind of signals introduced by fragment 1-83aa of Cpx, full-length Cpx, and mixture of 1-83 aa and 83-134 aa with various ratios. With the increase of CTD's concentration, the proportion of C-terminal-blocked state and middle-clamped state increases, meanwhile the proportion of the linker-open state decreases. When the ratio reaches 1:3, the types of signals and the signal portion are identical to those for the full length CpxI.

Interestingly, the proportion of C-terminal-blocked state and middle-clamped state increases with the ramping up of concentration of CpxI CTD fragment, meanwhile the proportion of the linker-open state decreases (Fig. 5c). Remarkably, more SNARE complexes were clamped to the middle-clamped state: they can't reassemble to a fully assembled complex, and need higher force to break the half-zippered state. Furthermore, the clamping function of Cpx can be reconstituted by fragment 1-83 aa of CpxI and its CTD as separate fragments in vitro (Fig. 5c, last two columns). Thus, physical continuity through the length of CpxI is not required to establish clamp function. CTD of CpxI inhibits the full zipper of SNARE complex, and plays an important role in the clamp function.

Discussion

The Ca^{2+}-triggered exocytosis of neurotransmitters and hormones is a tightly controlled process that has evolved to meet temporal precision and speed of intercellular communication. Cpx is likely the most controversially discussed SNARE-interacting proteins involved in exocytosis. The study of the regulatory mechanism of SNARE complex has important significance to complete the vesicle fusion theory, and guides the clinical treatment of the related diseases. The Ca^{2+}-triggered exocytosis could be triggered by interaction of multiple domains with the SNARE complex. Recall that the Cpx consists of four domains, NTD, AH, CH, and CTD. To examine the effect of CpxI on SNARE zippering, we observed a series of prominent long-dwelling states in the process of fast SNARE transition after the introduction of 8 μM full-length and different kinds of truncated CpxI. First, we found that the 1-83 aa of CpxI can powerfully stabilize the four helix-bundle of SNARE complex, and the 1-83 aa mainly implements the facilitate function, while the N-terminal domain (NTD) of CpxI plays a dominant role in this process. Second, the ability of CpxI to stabilize the SNARE complex critically depends on its NTD, which plays a dominant role of facilitate function. Third, a weak interaction occurred between individual CH and SNARE complex, since the proper and functional orientation needs the cooperation of other domains in CpxI. Fourth, CTD is mainly related to clamp function, and separate 1-83aa and C-terminal domain (CTD) of CpxI can efficiently reconstitute the inhibitory signal identical to that the full-length CpxI functions. Finally, multiple domains work cooperatively to ensure that a full-length Cpx works as a molecule switch — clamps the half-zippered SNARE

complex at the primed state of vesicle, and facilitates the SNARE complex zipper to fully-folded state when the trigger signal arrives in a physiological state (Fig. 6b).

Multiple domains in CpxI exert different functions on the dynamic zippering of SNARE complexes (Fig. 6). The above statistics are mainly based on the number of SNARE molecules changed after the introduction of CpxI. As control, we injected buffer though protein channel, and the majority (81% of 31 molecules under test) showed no change after the injection (first column of Fig. 6a). Once the fragment 83-134 aa (mostly part of CTD, without CH) was injected, and 18 of 27 SNARE complexes showed no change (second column of Fig. 6a), which was a negative control of experiments in Figure 5. For the column 3-5, we increased the concentration of CTD, the proportion of C-terminal-blocked state and middle-clamped state (clamp) increases, and probability of the liner-open state (facilitate) decreases with the abundance of the NTD.

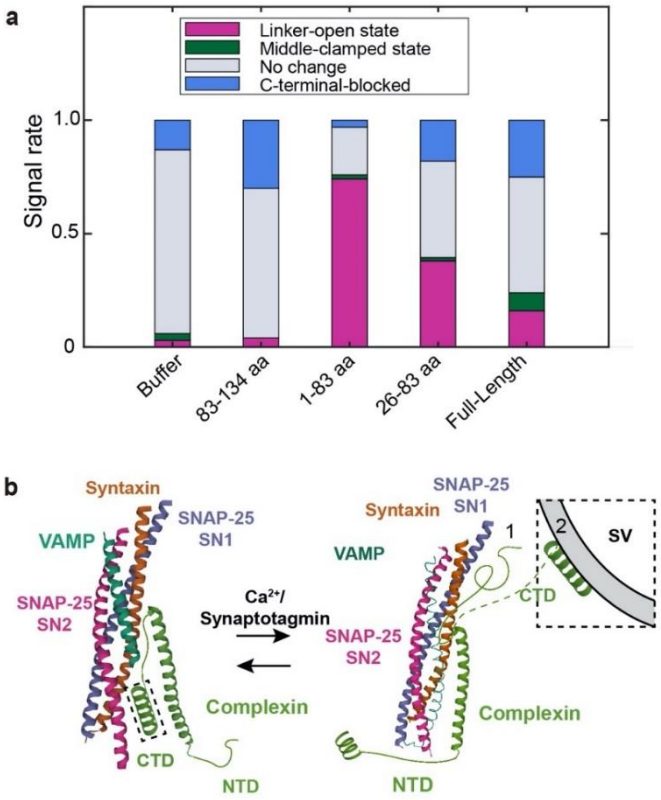

Figure 6. Function of the CpxI fragments on the dynamic zippering of SNARE complexes. a Summary of the signal rate of SNARE complex in presence of various truncations. With the increase of CTD concentration, the proportion of C-terminal-blocked state and middle-clamped state increases, and meanwhile with the increase of NTD abundance, the proportion of the linker-open state decreases. b Models of CpxI's two functions. Full-length CpxI clamps the SNARE complex into half-zippered state without Ca^{2+}, while CTD refold back to clamp at the time (CTD could be of helical conformation, shown in the black dashed box). Then NTD and Synaptotagmin help SNARE complex complete assembly in response to a triggering Ca^{2+}-stimulus in the physiological state, meanwhile stabilize the four-helix bundle of SNARE complex to

realize the neurotransmitter release. CTD of SNARE complex can be in free state (1) or member-binding state (2, dashed black box). Left (right) figure shows the PDB structure of 3RK3 (1KIL).

1-83 aa of CpxI is insufficient to the block the C-terminal zippering of SNARE complex compared with full-length CpxI, for the lack of CTD. Meanwhile, our complementary experiments suggest that separate N-and C-terminal domains of CpxI can efficiently reconstitute the clamp signal of the full-length CpxI (Figure 6a). This suggests that CTD of CpxI plays an active role in clamp function. Our single-molecule optical tweezers experiment has corroborated that the region with 26–83 aa in CpxI is the 'minimal clamping domain' of the protein [24,27]. The CpxI NTD have critical impact in the stable function of CpxI, while CpxI CTD plays an active role in fusion inhibition. In contradistinction, magnetic tweezers study has revealed that the unzipping of SNARE complexes occurred at higher force level by ~2 pN on average by interaction of CpxI with the pre-assembled SNARE complexes[28]. However, the SNARE complexes are not functional in the interaction of the CpxI and the pre-assembled SNARE. The vesicular release of mouse chromaffin cells suggests that the CpxI CTD exhibits a high degree of structural similarity to the C-terminal half of the SNAP25-SN1 domain and lowers the rate of SNARE complex formation in vitro[29]. The Cpx C-terminus competes with SNAP25-SN1 for binding to the SNARE complex and thereby halts progressive SNARE complex formation before the triggering of Ca^{2+}-stimulus [29]. Our study revealed that the rescue of the function of full-length Cpx requires a high concentration of CpxI CTD, and abundant CTD peptide is able to enhance the inhibitory function of

CpxI [29].

Our results on CpxI differ from those of the recent study of a single neuronal SNARE complex with complexin using magnetic tweezers[28]. In contrast to the stretching of the pre-assembled SNARE complex chaperoned with CpxI [28], single molecule optical tweezers experiment allows the study of the folding dynamics of SNARE complex in a functional state. First, the previous study using magnetic tweezers has reported that CpxI can clamp the SNARE complexes into "linker-open state" by adding complex to the pre-assembled SNARE complexes. However, they take these experiments by adding complexin to pre-assembled SNARE complex, which is not the functional state of SNARE complexes. We found that CpxI can introduce the "linker-open state", "middle-clamped state" and "C-terminal blocked state" by adding CpxI to individual SNARE complex when mimicking a real and functional dynamic transition, which can be reached by holding SNARE under constant average force at a fixed trap separation through optical tweezers.

Second, the previous study reported that the unzipping of SNARE complexes occurred at higher force levels by ~2 pN on average by adding complex, and they thought that the effects of mechanical tension on single SNARE complexes manifested only in a narrow range, namely between 13 and 16 pN. But we found the effect of CpxI can exist between 5-40 pN, which was clearly showed by our pulling experiments.

Thirdly, they show CpxI CH can also stabilize the four-helix bundle of SNARE complex, when we found CpxI CH could neither stabilize the SNARE complex nor

even functional binding to SNARE complex. In vitro analyses in Hela cells by Rothman and colleagues demarcated a region comprising amino acids 26–83 of CpxI as the 'minimal clamping domain' of the protein, which is consistent with our study.

Finally, they believed that the deletion of the C-terminal domain had no appreciable effect on any of the aspects of Cpx function, but our study first found the direct proof of CpxI CTD's active role in clamp function of fusion inhibition.

Overall, our results suggested that full-length CpxI performs as a calcium triggered molecular switch - clamp the SNARE complex into half-zippered state in the absence of Ca2+, and accelerates the SNARE complex complete assembly in response to a Ca2+-triggered stimulus in the physiological state.

Conclusion

In conclusion, we had built the dual-trap optical tweezers with differential detection and measured the significantly different folding kinetics of SNARE complexes in the absence and presence of both wild-type and mutant/truncated CpxI. To understand the function of the fragments of CpxI, and to elucidate the specific function unit, we synthesized a series of short fragments of CpxI and studied the interplay of each fragment with the SNARE assembly. In particular, the region 1-83 aa of CpxI can stabilize the four-helix bundle of SNARE motifs (facilitate), and the ability of CpxI to stabilize the SNARE complex critically depends on its NTD. Moreover, separate 1-83aa and C-terminal domains of CpxI can efficiently reconstitute the inhibitory signal of the full-length CpxI. Our single molecule optical tweezers experiment has

corroborated that the region with 26–83 aa in CpxI is the 'minimal clamping domain' of the protein [24,27]. The Cpx NTD have critical impact in the facilitate function of Cpx, while Cpx CTD plays an active role in clamp function. Collectively, our results delivered new insight into the fundamental mechanisms of Ca^{2+}-triggered exocytosis. For the precise realization of CpxI's function in vivo, a couple of other regulators (e.g., synaptotagmin) and phospholipid may participate in this process.

The mechanism of the dynamic interaction between the CpxI and the SNARE complex is just an example on how the dual trap optical tweezers applies mechanical tension and measures the dynamics of the protein folding. We anticipate that the dual-trap optical tweezers would further be applied to tackle the important disease, such as the Alzheimer's and Huntington's diseases, by tracing the minute misfolded state under mechanical tension. In combination of single molecule fluorescence resonance energy transfer (smFRET) [30], and Raman spectroscopy, optical tweezers will further greatly improve the dimension and SNR. Such tool would be more useful in biotechnology, nanoscience, and statistic physics in the single molecule level.

Materials and methods

Purification and labeling of proteins. The synaptic SNARE complex consists of VAMP2 (1-92, C2A, Q36C), syntaxin 1 (172-265, C173A, L209C), and SNAP25 (1-206). Substitution or truncation mutations in SNARE proteins and Cpx (C105A, 1-83, 26-83, 26-134, 83-134) were generated by overlap extension polymerase chain reaction

(PCR) using respective primers containing the desired non-homologous sequences [31]. All mutations were confirmed by DNA sequence analysis (BioSune, China). Genes corresponding to syntaxin and VAMP2 and the above Cpx were inserted into pET-SUMO vectors through TA-cloning. The proteins were then expressed in E. coli BL21(DE3) cells and purified as described in the manual of ChampionTM pET SUMO Expression System (Invitrogen). Typically, E. coli cell pellets were resuspended in 25 mM HEPES, 400 mM KCl, 10% Glycerol, 10 mM imidazole, pH 7.7 (25 mM HEPES, 800 mM NaCl, 5% Glycerol, 2 mM β-Me, 0.2% Triton X-100, pH 7.5 for Cpx) and broken up by sonication on ice to obtain clear cell lysates. The lysates were then cleared by centrifugation. The SNARE proteins in the supernatant were bound to Ni-NTA resin and washed by increasing imidazole concentrations up to 20 mM. The syntaxin protein was biotinylated in vitro by biotin ligase enzyme (BirA) as described (Avidity, CO). Finally, the His-SUMO tags on both proteins were cleaved directly on Ni-NTA resin by incubating the tagged SNARE proteins/resin slurry with SUMO protease (with a protein-to-protease mass ratio of 100:1) at 4℃ overnight. The SNARE proteins were collected in the flow-through while the His-SUMO tag was retained on the resin. SNAP25 was expressed from the pET-28a vector and purified through its N-terminal His-tag. All SNARE proteins were purified in the presence of 2 mM TCEP to avoid unwanted crosslinking. Peptides of Cpx (48-73) were synthetized by Yochem Biotech. All Cpx was transferred in the HEPES buffer (25 mM of HEPES, 50 mM NaCl, 0.02% CA630, pH 7.4) before optical tweezer experiment.

Formation and Crosslinking of SNARE complex. Ternary SNARE complexes were

formed by mixing syntaxin, SNAP25 and VAMP2 proteins with 3:4:5 molar ratios in 25 mM HEPES, 150 mM NaCl, 2 mM TCEP, pH 7.7 and the mixture was incubated at 4°C for 30 mins. Formation of the ternary complex was confirmed by SDS polyacrylamide gel electrophoresis. Excessive SNARE monomers or binary complexes were removed from the ternary complex by further purification through Ni-NTA resin using the His-Tag on the SNAP25 molecule. Middle intramolecular crosslinking around the -6-layer occurred at 34°C, 300 rpm, 16 h at a low concentration of 100 mM in phosphate buffer, 0.5 M NaCl, pH 8.5 without TCEP. Then the 2,260-bp DNA handle containing an activated thiol group at its 5' end was added to the solution of SNARE complex, which was just concentrated to more than 70 μM, with a SNARE complex to DNA handle molar ratio of 20:1. Intermolecular crosslinking occurred in open air between VAMP2 and the DNA handle, respectively, in 100 mM phosphate buffer, 0.5 M NaCl, pH 8.5. The DNA handle also contains two digoxigenin moieties at the other end. Both the thiol group and Digoxigenin moieties on the handle were introduced in the PCR reaction through primers. The excess of SNARE complexes in the crosslinking mixture was removed after the SNARE complex-DNA conjugates were bound to the anti-digoxigenin coated beads.

Single-molecule optical tweezers experiments. The high-resolution dual-trap optical tweezers were built by splitting a 1064 nm infrared laser (Spectra Physics) with orthogonal polarization. The optical tweezers were installed on the basement of the Molecular Imaging System in National Facility for Protein Sciences Shanghai with concrete background to isolate from the low-frequency vibration. The instrument was

also isolated from all the environmental noise including the fan from the laser controller, and all the operation were performed outside the isolated room after the samples were loaded to the microfluidics. Specifically, one trap was kept fixed, while the other is steered by a piezo mirror (MadCity labs). Despite movable, the beam spot on the back focal plane of the objectives is stationary with intensity distribution depending on the trapped microsphere position. Therefore, the optical tweezers can be calibrated through the power spectrum density of the positional signals,

$$|\tilde{x}(f)|^2 = \frac{k_B T}{c\pi^2\beta\left[\left(\frac{\alpha}{2\pi\beta}\right)^2 + f^2\right]} \qquad (1)$$

Here, α is the force constant, typically ranging in 0.01~0.8 pN/nm in our experiment, the conversion constant c is between 0.1~3 mV/nm, and $\beta = 6\pi r\eta$ is a known drag coefficient. Experiments were carried out at room temperature (22 °C) in the HEPES buffer (25 mM of HEPES, 50 mM NaCl, 0.02% CA630, pH 7.4), supplemented with oxygen scavenging system[32]. The first anti-digoxigenin antibody-coated polystyrene bead (diameter 2.12 μm) suspension was mixed with an aliquot of the mixture (crosslinked DNA handle and the SNARE complex), and the first bead is held in the right optical trap; the second bead (diameter 1.76 μm) coated with Streptavidin, was subsequently captured in another optical trap and brought close to the first bead to form the protein-DNA tether between two beads. Data were acquired at 20 kHz, mean-filtered in situ to 10 kHz, and saved on a computer disk for off-line analysis. In the pulling-relaxation experiment, single SNARE complexes were pulled (relaxed) by increasing (decreasing) the trap separation at a constant speed of 10 nm/sec. For

dynamics measurement, the separation of the traps was kept constant to record the temporal traces with stochastic transition.

Trap Geometry. The extension of the protein-DNA handle tether, X, is the sum of the extensions of the DNA handle, xDNA, the unfolded polypeptide portion of SNARE complex, xp, and the core structure, h, i.e.,

$$X = x_{DNA} + x_p + h, \qquad (2)$$

where h is assumed as the spatial length of the folded portion (such as coiled coil) projected along pulling direction, which also makes contribution to the final extension. In the fully folded state (native state), $h_0 = 2$ nm is determined from the x-ray structure of the protein[17], whereas for the fully unfolded state, $h = 0$. And when pulled in an axial direction, $h = 0.15 \times N_s \ nm$, where N_s is the number of amino acids in the folded portion and $0.15 \ nm$ is the helical rise of an amino acid along the helix axis.

According to the experiment, the stretching force F and protein-DNA handle tether X between the inner faces of two polystyrene beads follows,

$$D = X + \frac{F}{k_{\text{trap}}} + R_1 + R_2, \qquad (3)$$

where $k_{trap} = \frac{k_1 k_2}{k_1 + k_2}$ is the effective trap stiffness, R_1 and R_2 are the radii of two trapped polystyrene beads and D is the trap separation. The stretching force F, the extension X, the beads radii R_1 and R_2, the trap stiffness k_1 and k_2, the DNA contour length, LDNA=768 nm, and the trap separation D can be obtained from the

experiment.

FEC and dynamics fitting. To characterize the change in contour length of the SNARE-Cpx complex, unfolding and refolding traces were fitted to the worm-like chain model. For the DNA handle, the extension x_{DNA} as a function of the stretching force F is described by the Marko-Siggia model [33,34],

$$F = \frac{k_B T}{P_{DNA}}\left[\frac{1}{4(1-\frac{x_{DNA}}{L_{DNA}})^2} + \frac{x_{DNA}}{L_{DNA}} - \frac{1}{4}\right], \quad (4)$$

where PDNA and LDNA are the persistent and contour lengths of dsDNA, respectively, and kB is the Boltzmann constant. Similarly, the force for the unfolded polypeptide portion of SNARE complex can be formulated as

$$F = \frac{k_B T}{P_P}\left[\frac{1}{4(1-\frac{x_p}{l_p})^2} + \frac{x_p}{l_p} - \frac{1}{4}\right], \quad (5)$$

where F and x_{P} are the tension and extension of unfolded polypeptide respectively. The contour length of unfolded polypeptide l_p is related to the number N of amino acid in the polypeptide, which is described as l_p =0.4 x N, where 0.4 nm is the crystallographic contour length per amino acid [35,36]. And Pp is the persistence length of unfolded polypeptide. $k_{\mathrm{B}}T = 4.1\ pN \cdot nm$ is the energy unit at room temperature.

To characterize the folding pathway of protein, the extension of the SNARE complex in each state is calculated by the model. For each state, the extension consists of two parts: the extension of unfolded polypeptide l_{ir} (i= 1, 2, 3, or 4), which can be calculated by the Marko-Siggia formula and the extension of the folded portion. As described above, except for l_{P}, PDNA and P_{P}, all the other parameters in equations (1)-(4) can be

obtained experimentally or theoretically. Therefore, we could fit the experimental extension against the force range of each region (or each state) in FEC, to obtain their best-fit values. The fitting is performed after the FECs are mean-filtered using a time window of 11 ms. The persistence length PDNA and PP are different more or less for each molecule, so we firstly confirm these two parameters before each FEC fitting of each sample. The FEC region of fully unfolded state is firstly fitted with PDNA (10-50 nm) and PP (0.5-0.9 nm) as fitting parameters, while the known contour length of fully unfolded protein is taken as fixed parameter. Then the best-fit PDNA and PP values are utilized as fixed parameters in other FEC regions or states, in which the contour length l_P is to be fitted. Therefore, given the parameters of persistence length of DNA and protein, the structure information of proteins can be derived from fitted contour length of unfolded polypeptide according to equations (2)-(5).

The HMM analysis was normally performed on the whole extension-time trajectory (typically lasted 1–200 s), after the trajectory was mean-filtered to 5 kHz or 1 kHz. We evaluated the number of states by fitting the histogram distribution of the extension with multiple Gaussian functions. Then, the fitting parameters were further optimized in the HMM with a four-state transition model using gradient descent. The HMM analyses yielded the corresponding best-fit parameters from the experimental traces, such as the equilibrium force, and the extension change.

Supporting Information

Supporting Information is available from the Wiley Online Library.

Acknowledgements

We thank the National Center for Protein Science in Shanghai for use of the instrument. T. H. acknowledges Dr. Y. Gao for help on the SNARE assembly, and single molecule experiment. This work was supported by National Natural Science Foundation of China (31571346, 31771432).

Data availability

The data that support the findings of this study are available from the corresponding author upon reasonable request.

Competing interests

The authors declare no competing financial interests.

Author Contributions

T. H., N. F., and F. G. purified the protein, and collected the single molecule data; T. H., N. F., Y.Y. and Y. R. analyzed the data; Y. R., F. G. and Y. Y. built the instrument; J. L. provided overall guidance and support; T. H. and Y. R. drafted the manuscript, and all authors revised the manuscript.

References

1 Sudhof, T. C. Neurotransmitter release: the last millisecond in the life of a synaptic vesicle. *Neuron* **80**, 675-690, doi:10.1016/j.neuron.2013.10.022 (2013).

2 Poirier, M. A. *et al.* The synaptic SNARE complex is a parallel four-stranded helical bundle. *Nature Structural Biology* **5**, 765-769, doi:Doi 10.1038/1799 (1998).

3 Rizo, J. & Xu, J. The Synaptic Vesicle Release Machinery. *Annual review of*

biophysics **44**, 339-367, doi:10.1146/annurev-biophys-060414-034057 (2015).

4 Pobbati, A. V., Stein, A. & Fasshauer, D. N- to C-terminal SNARE complex assembly promotes rapid membrane fusion. *Science* **313**, 673-676, doi:10.1126/science.1129486 (2006).

5 Weninger, K., Bowen, M. E., Chu, S. & Brunger, A. T. Single-molecule studies of SNARE complex assembly reveal parallel and antiparallel configurations. *P Natl Acad Sci USA* **100**, 14800-14805, doi:10.1073/pnas.2036428100 (2003).

6 Gao, Y. *et al.* Single reconstituted neuronal SNARE complexes zipper in three distinct stages. *Science* **337**, 1340-1343, doi:10.1126/science.1224492 (2012).

7 Sudhof, T. C. & Rothman, J. E. Membrane Fusion: Grappling with SNARE and SM Proteins. *Science* **323**, 474-477, doi:10.1126/science.1161748 (2009).

8 Mcmahon, H. T., Missler, M., Li, C. & Sudhof, T. C. Complexins - Cytosolic Proteins That Regulate Snap Receptor Function. *Cell* **83**, 111-119, doi:Doi 10.1016/0092-8674(95)90239-2 (1995).

9 Trimbuch, T. & Rosenmund, C. Should I stop or should I go? The role of complexin in neurotransmitter release. *Nat Rev Neurosci* **17**, 118-125, doi:10.1038/nrn.2015.16 (2016).

10 Ma, L. *et al.* Munc18-1-regulated stage-wise SNARE assembly underlying synaptic exocytosis. *Elife* **4**, doi:10.7554/eLife.09580 (2015).

11 Sirinakis, G., Ren, Y. X., Gao, Y., Xi, Z. Q. & Zhang, Y. L. Combined versatile high-resolution optical tweezers and single-molecule fluorescence microscopy. *Rev Sci Instrum* **83**, doi:Artn 093708, 10.1063/1.4752190 (2012).

12 Finer, J. T., Simmons, R. M. & Spudich, J. A. Single myosin molecule mechanics: piconewton forces and nanometre steps. *Nature* **368**, 113-119, doi:10.1038/368113a0 (1994).

13 Moffitt, J. R., Chemla, Y. R., Izhaky, D. & Bustamante, C. Differential detection of dual traps improves the spatial resolution of optical tweezers. *Proc Natl Acad Sci USA* **103**, 9006-9011, doi:10.1073/pnas.0603342103 (2006).

14 Gittes, F. & Schmidt, C. F. Interference model for back-focal-plane displacement detection in optical tweezers. *Opt Lett* **23**, 7-9, doi:10.1364/ol.23.000007 (1998).

15 Zhang, Y. Energetics, kinetics, and pathway of SNARE folding and assembly revealed by optical tweezers. *Protein science : a publication of the Protein Society* **26**, 1252-1265, doi:10.1002/pro.3116 (2017).

16 Bouchiat, C. *et al.* Estimating the persistence length of a worm-like chain molecule from force-extension measurements. *Biophys J* **76**, 409-413, doi:10.1016/s0006-3495(99)77207-3 (1999).

17 Chen, X. C. *et al.* Three-dimensional structure of the complexin/SNARE complex. *Neuron* **33**, 397-409, doi:Doi 10.1016/S0896-6273(02)00583-4 (2002).

18 Bracher, A., Kadlec, J., Betz, H. & Weissenhorn, W. X-ray structure of a neuronal complexin-SNARE complex from squid. *J Biol Chem* **277**, 26517-26523, doi:10.1074/jbc.M203460200 (2002).

19 Choi, U. B., Zhao, M. L., Zhang, Y. X., Lai, Y. & Brunger, A. T. Complexin induces a conformational change at the membrane-proximal C-terminal end of

the SNARE complex. *Elife* **5**, doi:ARTN e16886, 10.7554/eLife.16886 (2016).

20 Xue, M. *et al.* Binding of the complexin N terminus to the SNARE complex potentiates synaptic-vesicle fusogenicity. *Nature structural & molecular biology* **17**, 568-575, doi:10.1038/nsmb.1791 (2010).

21 Maximov, A., Tang, J., Yang, X. F., Pang, Z. P. P. & Sudhof, T. C. Complexin Controls the Force Transfer from SNARE Complexes to Membranes in Fusion. *Science* **323**, 516-521, doi:10.1126/science.1166505 (2009).

22 Xue, M. *et al.* Distinct domains of complexin I differentially regulate neurotransmitter release. *Nature structural & molecular biology* **14**, 949-958, doi:10.1038/nsmb1292 (2007).

23 Kummel, D. *et al.* Complexin cross-links prefusion SNAREs into a zigzag array. *Nat Struct Mol Biol* **18**, 927-933, doi:10.1038/nsmb.2101 (2011).

24 Giraudo, C. G. *et al.* Distinct domains of complexins bind SNARE complexes and clamp fusion in vitro. *J Biol Chem* **283**, 21211-21219, doi:10.1074/jbc.M803478200 (2008).

25 Snead, D. *et al.* Unique Structural Features of Membrane-Bound C-Terminal Domain Motifs Modulate Complexin Inhibitory Function. *Frontiers in molecular neuroscience* **10**, 154, doi:10.3389/fnmol.2017.00154 (2017).

26 Wragg, R. T. *et al.* Evolutionary Divergence of the C-terminal Domain of Complexin Accounts for Functional Disparities between Vertebrate and Invertebrate Complexins. *Frontiers in molecular neuroscience* **10**, doi:ARTN 146, 10.3389/fnmol.2017.00146 (2017).

27 Giraudo, C. G. *et al.* Alternative zippering as an on-off switch for SNARE-mediated fusion. *Science* **323**, 512-516, doi:10.1126/science.1166500 (2009).

28 Shon, M. J., Kim, H. & Yoon, T. Y. Focused clamping of a single neuronal SNARE complex by complexin under high mechanical tension. *Nat Commun* **9**, doi:ARTN 3639, 10.1038/s41467-018-06122-3 (2018).

29 Makke, M. *et al.* A mechanism for exocytotic arrest by the Complexin C-terminus. *Elife* **7**, doi:ARTN e38981, 10.7554/eLife.38981 (2018).

30 Roy, R., Hohng, S. & Ha, T. A practical guide to single-molecule FRET. *Nature Methods* **5**, 507-516, doi:10.1038/nmeth.1208 (2008).

31 Higuchi, K. *et al.* Tissue-specific expression of apolipoprotein A-I (ApoA-I) is regulated by the 5'-flanking region of the human ApoA-I gene. *J Biol Chem* **263**, 18530-18536 (1988).

32 Woodside, M. T. *et al.* Direct measurement of the full, sequence-dependent folding landscape of a nucleic acid. *Science* **314**, 1001-1004, doi:10.1126/science.1133601 (2006).

33 Marko, J. F. & Siggia, E. D. Stretching DNA. *Macromolecules* **28**, 8759-8770, doi:DOI 10.1021/ma00130a008 (1995).

34 Bustamante, C., Marko, J. F., Siggia, E. D. & Smith, S. Entropic Elasticity of Lambda-Phage DNA. *Science* **265**, 1599-1600, doi:DOI 10.1126/science.8079175 (1994).

35 Stigler, J., Ziegler, F., Gieseke, A., Gebhardt, J. C. M. & Rief, M. The Complex Folding Network of Single Calmodulin Molecules. *Science* **334**, 512-516,

doi:10.1126/science.1207598 (2011).

36 Cecconi, C., Shank, E. A., Bustamante, C. & Marqusee, S. Direct observation of the three-state folding of a single protein molecule. *Science* **309**, 2057-2060, doi:10.1126/science.1116702 (2005).

Supplementary Files

This is a list of supplementary files associated with this preprint. Click to download.

- SupplementaryInformation.pdf